

FULL PAPER

Open Access



# In-orbit recalibration of Longwave Infrared Camera onboard Akatsuki

Makoto Taguchi<sup>1\*</sup> , Toru Kouyama<sup>2</sup> , Temma Sugawa<sup>3</sup>, Shin-ya Murakami<sup>4</sup> and Masahiko Futaguchi<sup>5</sup>

## Abstract

Akatsuki has been in operation since Venus orbit insertion-revenge 1 (VOI-R1) in December 2015 and has been making observations of Venus' cloud-top temperature with Longwave Infrared Camera (LIR) since the start of nominal observations in April 2016. LIR was originally designed to maintain its performance for at least 4 years after the VOI originally planned in December 2010. Although the operation time of LIR has exceeded its designed lifetime as of August 2022, it is still functioning normally. The mechanical shutter plate has been kept at a normal temperature and used as a hot reference in determining the brightness temperature of objects when in the closed position. Since the observed temperature of the background deep space is merely a value representing the output for no radiation input, it should be the same in any observation. This was around 180 K just after the launch of Akatsuki in May 2010; however, it has gradually increased to approximately 200 K by February 2022. Average Venus disk temperatures also show a slight increasing trend. The increases of the background and Venus' disk temperatures are most likely due to degradation of the sensitivity of the bolometer array used in LIR as an image sensor. These temperatures have apparently been increasing since LIR was activated in October 2016. While LIR is activated, the bolometer temperature is kept at 40 °C and a moderate baking effect may have accelerated degassing in the bolometer package, and the resulting increase of thermal conductivity or decrease of transmittance of the window contaminated by evaporated components may have degraded the sensitivity of the bolometer. A sensitivity degradation of 5% from October 2016 to February 2022 is estimated from the increasing trend of the background temperature. A correction has been made to the LIR data to keep the background temperature constant. The corrected data show no increasing trend in either the background or Venus' disk temperature. The corrected data are open to the public as a more reliable dataset for investigating the long-term variability of thermal condition at cloud-top altitudes.

**Keywords** Calibration, Brightness temperature, Venusian atmosphere, Thermal infrared camera, Micro-bolometer array

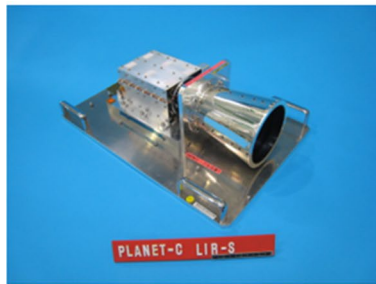
\*Correspondence:

Makoto Taguchi

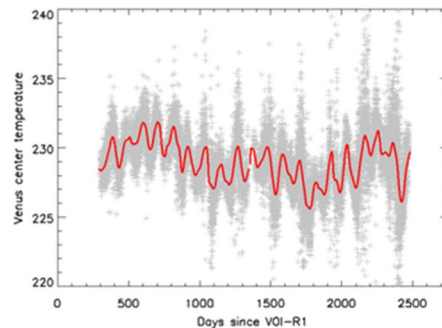
taguchi@rikkyo.ac.jp

Full list of author information is available at the end of the article

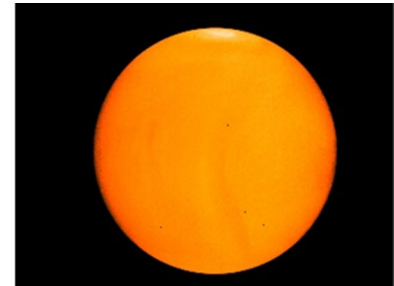
## Graphical Abstract



**Akatsuki/LIR-S**



**Temporal variation of the temperature of Venus' disk center for 7 years since VOI-R1**



**A brightness temperature image of Venus obtained by LIR at 20:00:12 UT on September 4, 2022**

## Main text

### Introduction

The Venus orbiter Akatsuki has been orbiting around Venus since December 2015 when Venus orbit insertion-revenge 1 (VOI-R1) was successful (Nakamura et al. 2016). The main purpose of the Akatsuki mission is to understand the dynamics of the Venusian atmosphere, especially the mechanism of the superrotation, namely, the strong zonal winds that are much faster than the rotation speed of Venus (Nakamura et al. 2011). Five cameras and a radio occultation instrument are aboard Akatsuki to visualize the three-dimensional structure of the Venusian atmosphere. Longwave Infrared Camera (LIR) is one of the optical instruments, acquiring brightness temperature distributions of the cloud tops. The sensing altitudes of LIR are estimated from a model atmosphere in which vertical distributions of temperature, minor gas species, and cloud particles are reconstructed from past observations, giving an altitude range from  $\sim 65$  km in low latitudes to  $\sim 60$  km in the polar region (Akiba et al. 2021).

Fukuhara et al. (2011) closely describes the principle, structure, and function of LIR. Since the micro-bolometer array used as an infrared image sensor in LIR needs no cooling apparatus, LIR is a light, small, and low-power-consuming instrument. LIR captures thermal emission from a target as a variation of the amount of electric resistance at each bolometer element (Tanaka et al. 2000), the response of which is linearly proportional to the intensity of the incident thermal emission. A mechanical shutter attached to LIR functions as an optical shutter to prevent direct exposure of the image sensor to intense solar radiation and also as a reference black body to derive a target temperature. Because the bolometer array used in LIR has a wide variation in

the pixel bias level, LIR captures a pair of shutter and object images in each image acquisition sequence to cancel the pixel bias by subtracting the shutter image from the object image. In addition, to use each shutter image as a reference temperature image, the temperature of the shutter is controlled around 297 K (24 °C). Then, each pixel value in the subtracted image is converted to the corresponding intensity of the thermal emission using parameters obtained in ground-based experiments, as described in Fukuhara et al. (2011). Finally, the obtained thermal emission is converted to the corresponding temperature based on Planck's law of blackbody radiation.

The temperature of the bolometer is stabilized at 313 K (40 °C) while LIR is activated. Calibration data were obtained during the prelaunch test for the expected range of shutter temperature variation, and the dependence of an output brightness temperature on the shutter temperature is corrected in a data processing pipeline of LIR. The noise equivalent temperature difference (NETD) or the temperature resolution of LIR is 0.3 K. This means a pixel-to-pixel difference in output brightness temperatures of 0.3 K or larger in an image can be detected. On the other hand, the accuracy of absolute temperature measurement of LIR is 3 K (Fukuhara et al. 2011).

An unexpected dependence of the brightness temperature of the Venus disk on the temperature of the hood of LIR was found after VOI-R1. A part of the infrared radiation emitted from the hood heated by solar radiation is absorbed by the lens, which then also emits more infrared radiation than expected in the calibration procedure that is absorbed by the bolometer to be a source of output bias. A dataset corrected for the hood temperature dependence has been released (Fukuhara et al. 2017a).

Several important findings about the thermal structure at the cloud tops of Venus have been reported as results of investigations using data obtained by LIR. The first Venus full-disk image obtained by LIR after VOI-R1 exhibited a pronounced bow-shaped thermal structure, which was later identified as a temperature variation induced by a stationary gravity wave excited deep in the lower atmosphere close to the surface of high land in the low-latitude region and propagating upward to the cloud top (Fukuhara et al. 2017b; Kouyama et al. 2017; Fukuya et al. 2022). Because of the ability of LIR to measure brightness temperature in both the dayside and nightside with equal quality, it is possible to generate an image of the global structure of thermal tides, including the three-dimensional structure by utilizing the emission angle dependence of the sensing altitudes of LIR (Kouyama et al. 2019; Akiba et al. 2021). Horizontal wind fields derived by a cloud tracking method from ultraviolet images obtained by the Ultraviolet Imager (UVI) onboard Akatsuki together with brightness temperature distributions obtained by LIR revealed that the superrotation is maintained by vertical and horizontal angular momentum transport toward the equatorial cloud-top altitudes by the thermal tides (Horinouchi et al. 2020). A cloud tracking method was also applied to brightness temperature images and it was found that a meridional component of a horizontal wind at the cloud tops in the nightside is equatorward, opposite to that in the dayside (Fukuya et al. 2021). Kajiwara et al. (2021) reported planetary-scale waves extracted from brightness temperature distributions at the cloud tops, indicating that there exist Kelvin and Rossby waves with periods of several days.

Brightness temperature data over six earth years or ten Venus years have been accumulated, which is long enough to study the climatology of the cloud-top thermal conditions, secular variations of the thermal budget of Venus, and variations in various wave activities with long periods. However, most of these studies have not yet been undertaken because the accuracy of the absolute brightness temperature derived by LIR is insufficient.

Although LIR has no precise internal calibration black body, the shutter plate is used as a simple hot calibration source for the higher temperature reference. The background deep space temperature is necessarily constant and can be used as a precise lower temperature reference. However, we confirmed that the background temperature shows a gradual increase during the whole period of LIR observation of more than 20 K over five earth years, which is likely due to a calibration issue. An increasing trend is also confirmed in Venus' disk temperature, though the magnitude of this trend is smaller than that for the background temperature. To improve the accuracy of absolute brightness temperature measurements, a

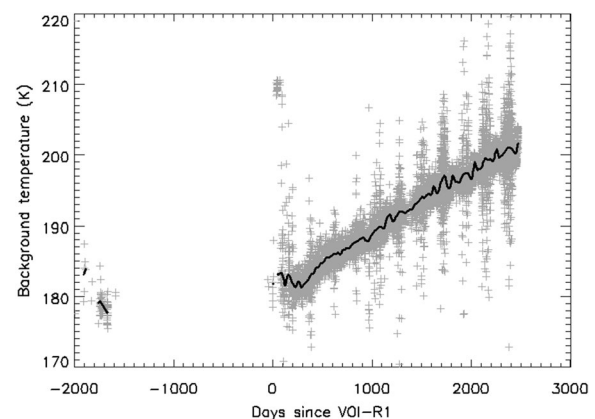


**Fig. 1** Temporal variation of background deep space temperature from the launch of Akatsuki to February 2022. Running mean values are shown by a solid line

method for correcting the brightness temperature using the background temperature has been developed and applied to the data. This paper presents the correction method and reports the long-term variation of Venus' disk temperature using the corrected data.

#### Long-term variation of background and Venus' disk temperatures

Figure 1 shows the background deep space temperature derived from the brightness temperature images archived as the L2c data of LIR (Murakami et al. 2017). It is noted that almost no data are available during the interplanetary cruising period between VOI in December 2010 (1826 days before VOI-R1) and VOI-R1 because LIR was mostly turned off. The figure clearly shows a linear increasing trend since LIR was regularly turned on for stabilizing its thermal state since October 2016 (approximately 300 days after VOI-R1) (Fukuhara et al. 2017a, b).

Because a reference shutter image and a target object image are taken alternately in one LIR observation sequence, any variation in the bias level will be canceled by the subtracting procedure, even if there is a long-term increasing trend in the bias level in the LIR image. Another candidate cause for the increasing trend is sensitivity degradation of the LIR optical system. As described before, LIR measures the difference in the output between a temperature-controlled reference (shutter) and a target. If sensitivity degradation occurs, the difference between the outputs for the reference and target images reduces accordingly, as illustrated in Fig. 2. Since the reference temperature of the LIR shutter,  $\sim 297$  K ( $\sim 24$  °C), is higher than the temperature at the cloud-top level of Venus,  $\sim 230$  K, a reduction in the difference between the measured reference and target

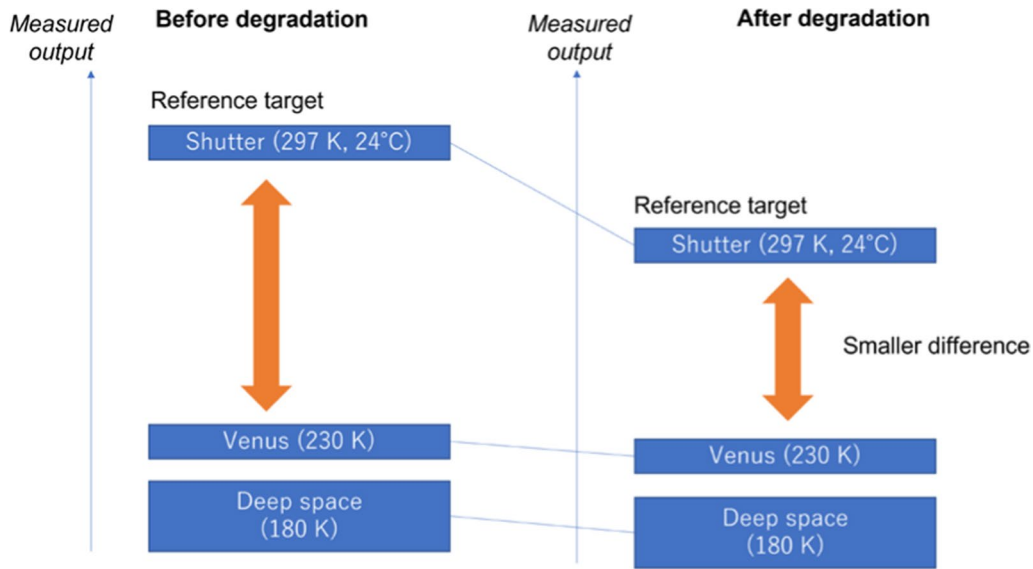


**Fig. 2** Schematic view of a change of output brightness temperature of Venus relative to temperatures of the shutter and deep space due to sensitivity degradation of LIR. It is noted that the deep space temperature is not a real temperature but an apparent temperature

outputs makes the measured target temperature hotter than the actual temperature.

We confirmed the occurrence of sensitivity degradation of LIR from further evidence in LIR images. On August 22, 2020, some pixels in the deep space region in an image were assigned an invalid value, which indicates that the outputs at those pixels in the raw target image were smaller than the lower limit of the dynamic range of LIR. This was not observed in the early phase of LIR observation and was observed more frequently in 2022, indicating that sensitivity degradation in the LIR optical system is progressing.

#### Correction of sensitivity degradation

The difference in the outputs of the reference and target images described in the previous sections is important for temperature measurements by LIR. We assume that the sensitivity degradation linearly affects the outputs, but, because the shutter temperature is used as a reference temperature, it does not affect the output when LIR observes a target with the same temperature as the shutter temperature. The observed radiance,  $I_o(T, t)$ , for a target temperature,  $T$ , at a time,  $t$ , can be represented as

$$I_o(T, t) = (1 + \alpha(t'))(I(T) - I(T_s)) + I(T_s), \quad (1)$$

where  $I(T)$  represents blackbody radiation as a function of the target temperature,  $T_s$  is the shutter temperature, and  $\alpha(t')$  represents the magnitude of the sensitivity variation as a function of integrated duration of LIR turned on,  $t'$ . It is noted that for evaluating  $I$  from  $T$  and  $T$  from  $I$ , an approximation is used to reduce computation cost

in the data processing pipeline (Fukuhara et al. 2017a, and Appendix).

For the degradation case,  $\alpha(t')$  should be negative, and the degradation can be ignored at  $t' = 0$ ; thus,

$$\alpha(0) = 0. \quad (2)$$

By letting  $\Delta I_b(t, t_0)$  be the difference of observed radiance of deep space at  $t$  and at the time when the degradation can be ignored ( $t_0$ ),  $\Delta I_b(t, t_0)$  can be evaluated using (1) as

$$\begin{aligned} \Delta I_b(t, t_0) &\equiv I_o(T_b, t) - I_o(T_b, t_0) \\ &= I_o(T_b, t) - I(T_b) \\ &= \alpha(t')(I(T_b) - I(T_s)), \end{aligned} \quad (3)$$

where  $T_b$  is the apparent temperature of the deep space. Then, from (3), the amount of sensitivity degradation can be measured as

$$\alpha(t') = \frac{\Delta I_b(t, t_0)}{I(T_b) - I(T_s)}. \quad (4)$$

As described in Fukuhara et al. (2011), in this study 297 K (24 °C) is used for  $T_s$  for evaluating  $I(T_s)$ . We used 181.4 K for  $T_b$  for evaluating the background intensity based on observation results in the cruise phase of Akatsuki (see Fig. 1) and providing zero degradation at  $t=0$  in a fitting procedure of a linear function (see the paragraphs below and Fig. 3). It is noted that  $T_b$  is the lower limit of LIR observation (Fukuhara et al. 2017a, b), and from the observation it could be up to 2 K uncertainty for



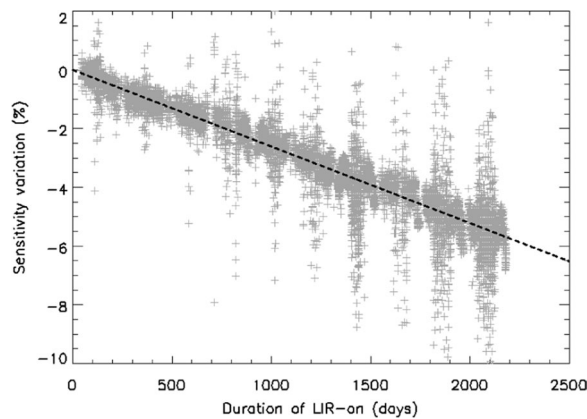


**Fig. 3** Sensitivity variation of LIR as a function of the duration of the LIR's operation, showing observations (gray crosses) and a fitted trend (dashed line). The negative values indicate degradation of sensitivity

determining the lower limit temperature, which affects the uncertainty in evaluation of the degradation.

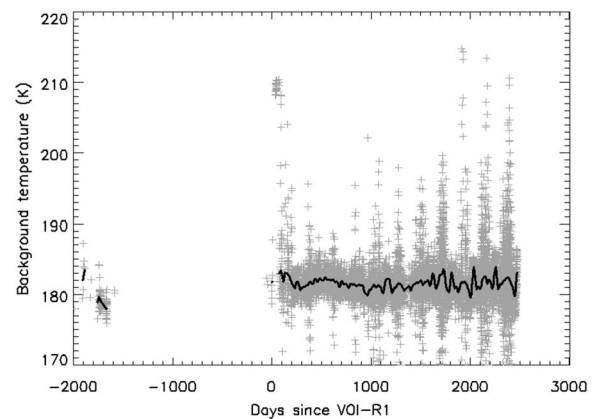
Then,  $\Delta I_b(t, t_0)$  can be evaluated from the observation results ( $I_o(T_b, t)$ ) shown in Fig. 1. It should be noted that it is not known whether the small fluctuations in the increasing trend seen in Fig. 1 were due to actual sensitivity variations or to other measurement errors. In this study, to cancel the major component of the temperature increasing trend, we simply modeled the increasing trend as a linear trend. More precise corrections should be discussed in a future work.

Figure 3 shows the estimated sensitivity degradation as a function of duration of the LIR-on. It indicates that a  $-2.617 \pm 0.037\%$  sensitivity degradation occurred within 1,000 days of duration of the LIR-on, and a more than 5% degradation occurred during the mission phase. The uncertainty shows an error range of  $3\sigma$  evaluated by considering an error of fitting a linear function to the sensitivity degradation and uncertainty in determining the background temperature ( $\pm 2$  K). From Fig. 3, the correction of the observed intensity of a target can be represented from (1) as

$$I(T) = \frac{I_o(T, t) - I(T_s)}{1 + \alpha(t')} + I(T_s). \quad (5)$$

Figure 4 shows the background temperature corrected from the observed background temperature shown in Fig. 1 based on (5), showing that the increasing trend was successfully canceled.

Same as the background deep space temperature, the increasing trend seen in Venus' disk temperature, which could reach 5–7 K, was also canceled after correcting for the degradation of the LIR sensitivity (Fig. 5).



**Fig. 4** The data in Fig. 1 after the correction for sensitivity degradation

## Discussion

Long-term degradation of passive electrical or optical parts is unlikely to be a cause of the sensitivity degradation of LIR. The Thermal Infrared Imager (TIR) onboard Hayabusa2, which is an infrared camera identical to the Akatsuki LIR except for its sensitive temperature range (Okada et al. 2017), showed a similar increase of dark counts during Hayabusa2's rendezvous with the asteroid Ryugu for 17 months while TIR was basically always turned on, but no increase of dark counts during the interplanetary cruise phases to and from Ryugu while TIR was turned off except for very short activations for in-flight tests (Hirabayashi et al. 2021). This fact supports the following speculation. When these cameras are activated, the bolometer temperature is kept at 313 K (40 °C) by a Peltier cooler/heater. The bolometer is sealed in an evacuated package for use under atmospheric pressure. Gentle baking of the bolometer at 313 K accelerates evaporation of materials in the bolometer package. The evaporated materials increase the thermal conductivity in the bolometer package or decrease the transmittance of a Ge window attached to the package by coagulation on the inner surface of the window. Either effect decreases the sensitivity of the bolometer, though a quantitative estimation is difficult.

The background temperature without correction shows a linear increasing trend with the integrated time of operation of LIR. It is currently not clear whether the background temperature will continue to increase or slow in its increase and converge to a certain value. Unfortunately, the end of the Akatsuki mission is not far off. However, the trend of the background temperature should be carefully monitored and, if necessary, an additional correction should be performed on the data.

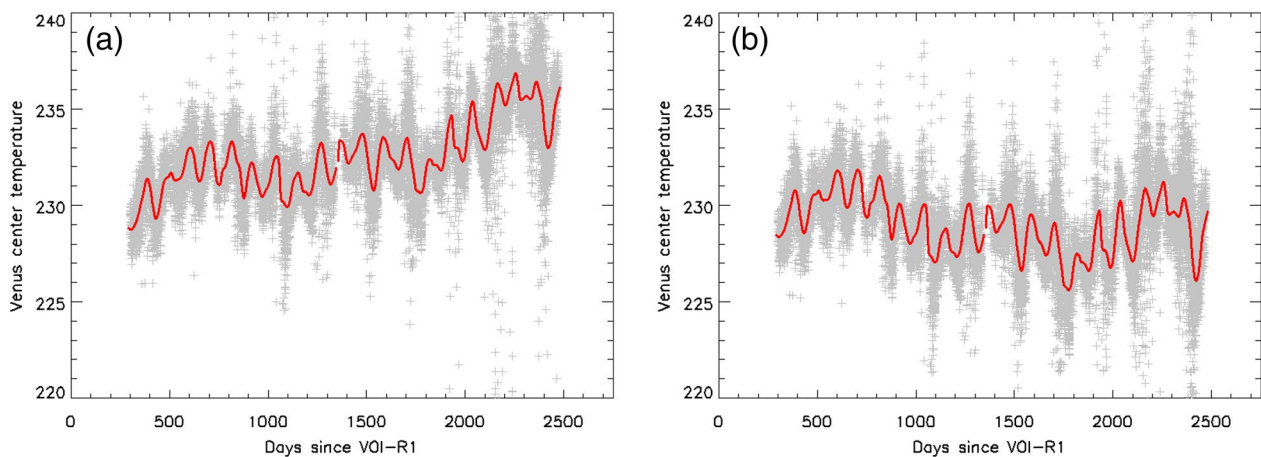


**Fig. 5** Temporal variations of the temperature of Venus' disk center **a** without and **b** with the correction. Running mean values are shown by red solid lines. The periodic variation of  $\sim 100$  days is due to a thermal tide component following the sub-spacecraft local time variation

## Conclusion

The increasing trend of the background temperature is likely due to sensitivity degradation of LIR, resulting in an apparent slight increase of the Venus disk temperature of 5 K. The rate of the sensitivity degradation is estimated to be  $-2.617 \pm 0.037\%/1000\text{days}$ . A method to correct the apparent variation of the brightness temperature using the background temperature is applied to all data obtained by LIR after VOI-R1. The long-term trend of the Venus disk temperature in the corrected dataset comprises various components of temperature variations presumably due to changes in the cloud distribution, albedo, or wave activity. The new dataset is open to the public for studies of the influence of these phenomena on the thermal environment at cloud tops.

## Appendix

In this section, we summarize approximations for converting observed brightness to corresponding brightness temperature and brightness temperature to observed brightness in the data processing pipeline of LIR, which was updated from Fukuhara et al. (2017a).

LIR captures integrated thermal brightness within a wavelength range approximately from 8 to 12  $\mu\text{m}$ . Because of the wavelength range, the conversion between observed brightness and corresponding brightness temperature requires a complex calculation of integration of Planck's law. In addition, this calculation is needed for every pixel. To avoid much calculation in the data processing pipeline, we adopt an approximation with a polynomial function (Fukuhara et al. 2017a).

At first, in the experiments for calibration of LIR before the launch, we used a temperature-controlled black

plate whose emissivity was known. By combining LIR's response, thermal radiation from the controlled black plate observed by LIR can be represented theoretically as

$$I = \int_{\lambda} \alpha(\lambda) B(T, \lambda) d\lambda, \quad (6)$$

where  $I$  is observed brightness by LIR,  $\lambda$  is a wavelength,  $\alpha(\lambda)$  is LIR's response as a function of wavelength, and  $B(T, \lambda)$  is blackbody radiation of temperature  $T$ . Here, a simple box car function

$$\alpha(\lambda) = \begin{cases} 1 & 8 \mu\text{m} \leq \lambda \leq 12 \mu\text{m} \\ 0 & \lambda < 8 \mu\text{m}, 12 \mu\text{m} < \lambda \end{cases} \quad (7)$$

was used in Fukuhara et al. (2017a). By considering transmittance of the lens, the filter and the window of the bolometer package, and spectral response of the bolometer, a more accurate response function shown in Fig. 6 has been adopted in the current data processing pipeline.

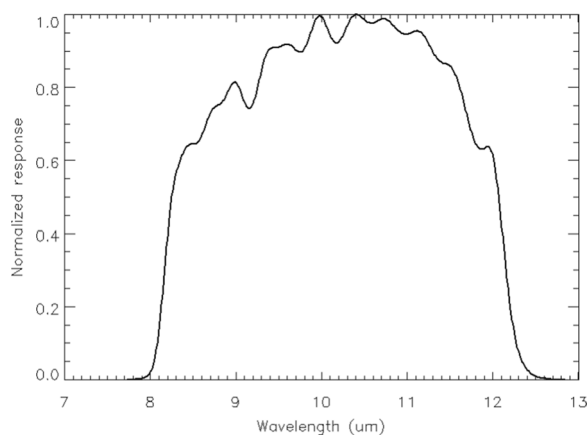
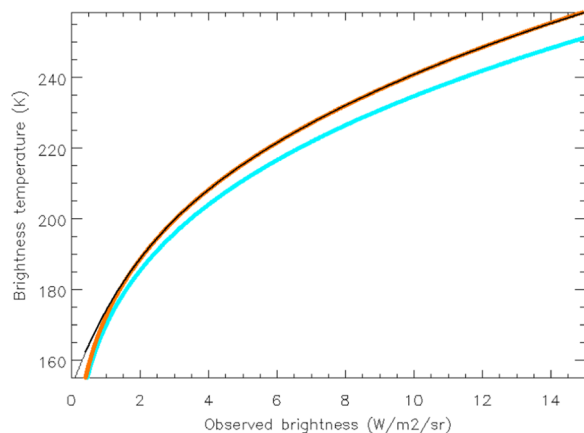
Then, as in Fukuhara et al. (2017a), a 7-degree polynomial function in terms of  $I$  is used to evaluate approximated brightness temperature,  $T'$ , as

$$T' = \sum_{i=0}^7 a_i I^i, \quad (8)$$

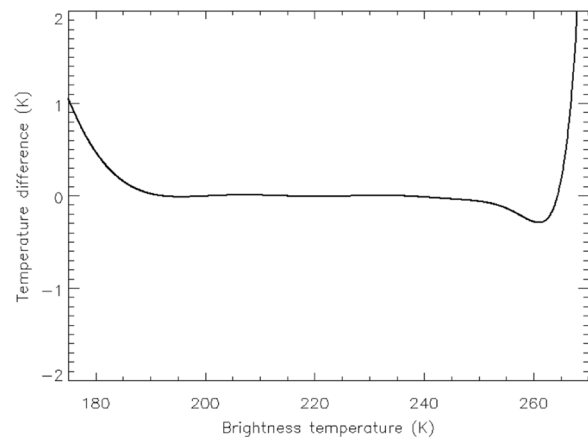
where  $a_i$  are coefficients for the approximation, which was evaluated from fitting the polynomial function to  $T$ . Figure 7 shows comparison of  $T$  and  $T'$  as functions of  $I$ , and Table 1 shows  $a_i$  used in the data processing in this study. It is noted that emissivity of an object from which thermal radiation is detected by LIR is assumed to be unity.

**Table 1** Actual values of coefficients  $a_i$ 

Coefficient	Value
$a_0$	152.4928
$a_1$	25.77792
$a_2$	-5.161996
$a_3$	0.8055189
$a_4$	-0.08148206
$a_5$	$5.02841 \times 10^{-3}$
$a_6$	$-1.714920 \times 10^{-4}$
$a_7$	$2.47000 \times 10^{-6}$

**Fig. 6** Normalized LIR's response as a function of wavelength**Fig. 7** Comparison of brightness temperatures derived with LIR's response approximated by the boxcar function (light blue) and with that shown in Fig. 6 (red). A black solid line indicates approximation of the temperature profile with a 7-degree polynomial function used in the data processing in this study

Difference of brightness temperature derived from the precise theoretical function  $T$  and that derived from the approximated function  $T'$  is shown in Fig. 8.

**Fig. 8** Difference of brightness temperatures derived from the precise theoretical function and the approximated function

The approximation is valid (difference of  $T$  and  $T'$  is less than 0.2 K) within a range of 190–260 K, which was determined to satisfy the science requirement of LIR. Although 180 K is out of the range, still the difference between  $T$  and  $T'$  is less than 0.5 K, and corresponding radiance is just less than  $0.02 \text{ W/m}^2/\text{sr}$ , which is much smaller than target brightness (more than  $1.5 \text{ W/m}^2/\text{sr}$  even for a 180 K target).

#### Abbreviations

LIR	Longwave Infrared Camera
NETD	Noise equivalent temperature difference
TIR	Thermal Infrared Imager
UVI	Ultraviolet Imager
VOI-R1	Venus orbit insertion-revenge 1

#### Acknowledgements

The authors would like to acknowledge all the members of the Akatsuki project team for their efforts in the Akatsuki operation.

#### Author contributions

MT and TK are the principal investigator and a co-investigator of LIR, respectively, and contributed to development of the data correction method. SM and MF contributed to construct the data processing pipeline of LIR. TS contributed to prepare the manuscript. All the authors read and approved the final manuscript.

#### Funding

This work was supported by JSPS KAKENHI Grant Numbers 15K17767, 16H02231, 19K14789, and 20H01958.

#### Availability of data and materials

The L2c LIR data are publicly available from the JAXA archive website, DARTS, and the NASA archive website, PDS (Murakami et al. 2017). Data products created by using the calibration procedure discussed in this paper will be opened to public as a part of the PDS4 Akatsuki LIR Bundle (Taguchi et al. 2023).

## Declarations

## Competing interests

The authors declare no competing financial interests.

## Author details

<sup>1</sup>College of Science, Rikkyo University, 3-34-1 Nishi-Ikebukuro, Toshima-Ku, Tokyo 171-8501, Japan. <sup>2</sup>Digital Architecture Research Center, National Institute of Advanced Industrial Science and Technology, 2-3-26 Aomi, Koto-Ku, Tokyo 135-0064, Japan. <sup>3</sup>Graduate School of Science, Rikkyo University, 3-34-1 Nishi-Ikebukuro, Toshima-Ku, Tokyo 171-8501, Japan. <sup>4</sup>Institute of Space and Astronautical Science, Japan Aerospace Exploration Agency, 3-1-1 Yoshinodai, Chuo-ku, Sagami, Kanagawa 252-5210, Japan. <sup>5</sup>Omori Medical Center, Toho University, 6-11-1 Omorinishi, Ota-ku, Tokyo 143-8541, Japan.

Received: 5 January 2023 Accepted: 9 March 2023

Published: 10 April 2023

## References

- Akiba M, Taguchi M, Fukuhara T, Imamura T, Kouyama T, Sato TM (2021) Thermal tides in the upper cloud layer of Venus as deduced from the emission angle dependence of the brightness temperature by Akatsuki/LIR. *J Geophys Res Planets* 126:e2020JE06808. <https://doi.org/10.1029/2020JE06808>
- Fukuhara T, Taguchi M, Imamura T, Nakamura M, Ueno M, Suzuki M, Iwagami N, Sato M, Mitsuyama K, Hashimoto GL, Ohshima R, Kouyama T, Ando H, Futaguchi M (2011) LIR: Longwave Infrared Camera onboard the Venus orbiter Akatsuki. *Earth Planets Space* 63:1009–1018. <https://doi.org/10.5047/eps.2011.06.019>
- Fukuhara T, Taguchi M, Imamura T, Hayashitani A, Yamada T, Futaguchi M, Kouyama T, Sato TM, Takamura M, Iwagami N, Nakamura M, Suzuki M, Ueno M, Hashimoto GL, Sato M, Takagi S, Yamazaki A, Yamada M, Murakami S, Yamamoto Y, Ogohara K, Ando H, Sugiyama K, Kashimura H, Ohtsuki S, Ishii N, Abe T, Satoh T, Hirose C, Hirata N (2017a) Absolute calibration of brightness temperature of the Venus disk observed by the Longwave Infrared Camera onboard Akatsuki. *Earth Planets Space* 69:141. <https://doi.org/10.1186/s40623-017-0727-y>
- Fukuhara T, Futaguchi M, Hashimoto GL, Horinouchi T, Imamura T, Iwagami N, Kouyama T, Murakami S, Nakamura M, Ogohara K, Sato M, Sato TM, Suzuki M, Taguchi M, Takagi S, Ueno M, Watanabe S, Yamada M, Yamazaki A (2017b) Large stationary gravity wave in the atmosphere of Venus. *Nat Geosci* 10:85–88. <https://doi.org/10.1038/NGEO2873>
- Fukuya K, Imamura T, Taguchi M, Kouyama T, Horinouchi T, Peralta J, Futaguchi M, Yamada T, Sato TM, Yamazaki A, Murakami S, Satoh T, Takagi M, Nakamura M (2021) The nightside cloud-top circulation of the atmosphere of Venus. *Nature* 595:511–515. <https://doi.org/10.1038/s41586-021-03636-7>
- Fukuya K, Imamura T, Taguchi M, Kouyama T (2022) Horizontal structures of bow-shaped mountain wave trains seen in thermal infrared images of Venusian clouds taken by Akatsuki LIR. *Icarus*. <https://doi.org/10.1016/j.icarus.2022.114936>
- Hirabayashi M, Mimasu Y, Sakatani N, Watanabe S, Tsuda Y, Saiki T, Kikuchi S, Kouyama T, Yoshikawa M, Tanaka S, Nakazawa S, Takei Y, Terui F, Takeuchi H, Fujii A, Iwata T, Tsumura K, Matsuura S, Shimaki Y, Urakawa S, Ishibashi Y, Hasegawa S, Ishiguro M, Kuroda D, Okumura S, Sugita S, Okada T, Kameda S, Kamata S, Higuchi A, Senshu H, Noda H, Matsumoto K, Suetsugu R, Hirai T, Kitazato K, Farnocchia D, Naidu SP, Tholen DJ, Hergenrother CW, Whiteley RJ, Moskovitz NA, Abell PA (2021) Hayabusa2 extended mission: New voyage to rendezvous with a small asteroid rotating with a short period. *Adv Space Res* 68:1533–1555. <https://doi.org/10.1016/j.jasr.2021.03.030>
- Horinouchi T, Hayashi Y, Watanabe S, Yamada M, Yamazaki A, Kouyama T, Taguchi M, Fukuhara T, Takagi M, Ogohara K, Murakami S, Peralta J, Limaye SS, Imamura T, Nakamura M, Sato TM, Satoh T (2020) How is the super-rotation of Venus' atmosphere maintained by waves and turbulence. *Science* 368:405–409. <https://doi.org/10.1126/science.aaz4439>
- Kajiwaru N, Imamura T, Taguchi M, Kouyama T (2021) Planetary-scale waves seen in thermal infrared images of Venusian cloud top. *J Geophys Res Planets* 126:e2021JE007047. <https://doi.org/10.1029/2021JE007047>
- Kouyama T, Imamura T, Taguchi M, Fukuhara T, Sato TM, Yamazaki A, Futaguchi M, Murakami S, Hashimoto GL, Ueno M, Iwagami N, Takagi S, Takamura M, Yamada T, Takagi M, Ogohara K, Kashimura H, Horinouchi T, Sato N, Yamada M, Yamamoto Y, Ohtsuki S, Sugiyama K, Ando H, Satoh T, Nakamura M (2017) Topographical and local-time dependence of large stationary gravity waves observed at the cloud top of Venus. *Geophys Res Lett* 44:12098–12105. <https://doi.org/10.1002/2017GL075792>
- Kouyama T, Taguchi M, Fukuhara T, Imamura T, Horinouchi T, Sato TM, Murakami S, Hashimoto GL, Lee Y-J, Futaguchi M, Yamada T, Akiba M, Satoh T, Nakamura M (2019) Global structure of thermal tides in the upper cloud layer of Venus revealed by LIR onboard Akatsuki. *Geophys Res Lett* 46:9457–9465. <https://doi.org/10.1029/2019GL083820>
- Murakami S, Kouyama T, Fukuhara T, Taguchi M, McGouldrick K, Yamamoto Y, Hashimoto GL (2017) Venus climate orbiter Akatsuki LIR calibrated data v10, VCO-V-LIR-3-CDR-V10. NASA Planet Data Syst. <https://doi.org/10.17597/ISAS.DARTS/VCO-00012>
- Nakamura M, Imamura T, Ishii N, Abe T, Satoh T, Suzuki M, Ueno M, Yamazaki A, Iwagami N, Watanabe S, Taguchi M, Fukuhara T, Takahashi Y, Yamada M, Hoshino N, Ohtsuki S, Uemizu K, Hashimoto GL, Takagi M, Matsuda Y, Ogohara K, Sato N, Kasaba Y, Kouyama T, Hirata N, Nakamura R, Yamamoto Y, Okada N, Horinouchi T, Yamamoto M, Hayashi Y (2011) Overview of Venus orbiter, Akatsuki. *Earth Planets Space* 63:443–457. <https://doi.org/10.5047/eps.2011.02.009>
- Nakamura M, Imamura T, Ishii N, Abe T, Kawakatsu Y, Hirose C, Satoh T, Suzuki M, Ueno M, Yamazaki A, Iwagami N, Watanabe S, Taguchi M, Fukuhara T, Takahashi Y, Yamada M, Imai M, Ohtsuki S, Uemizu K, Hashimoto GL, Takagi M, Matsuda Y, Ogohara K, Sato N, Kasaba Y, Kouyama T, Hirata N, Nakamura R, Yamamoto Y, Horinouchi T, Yamamoto M, Hayashi Y, Kashimura H, Sugiyama K, Sakanoi T, Ando H, Murakami S, Sato TM, Takagi S, Nakajima K, Peralta J, Lee Y-J, Nakatsuka J, Ichikawa T, Inoue K, Toda T, Toyota H, Tachikawa S, Narita S, Hayashiyama T, Hasegawa A, Kamata Y (2016) AKATSUKI returns to Venus. *Earth Planets Space* 68:75. <https://doi.org/10.1186/s40623-016-0457-6>
- Okada T, Fukuhara T, Tanaka S, Taguchi M, Imamura T, Arai T, Senshu H, Ogawa Y, Demura H, Kitazato K, Nakamura R, Kouyama T, Sekiguchi T, Hasegawa S, Matsunaga T, Wada T, Takita J, Sakatani N, Horikawa Y, Endo K, Helbert J, Mueller TG, Hagermann A (2017) Thermal infrared imaging experiments of C-Type asteroid 162173 Ryugu on Hayabusa2. *Space Sci Rev* 208:255–286. <https://doi.org/10.1007/s11214-016-0286-8>
- Taguchi M, Kouyama T, Futaguchi M, Sato TM, Yamada T, Murakami S, Yamada M, Yamazaki A, Ogohara K, Takagi M, Kashimura H, Horinouchi T, Imamura T, Yamamoto Y, Hashimoto GL, McGouldrick K (2023) Venus Climate Orbiter Akatsuki Longwave Infrared Camera Bundle v1.0. [urn:jaxa:darts:vco\\_lir](https://doi.org/10.17597/ISAS.darts/vco-00600). JAXA Data Archives and Transmission System. <https://doi.org/10.17597/ISAS.darts/vco-00600>
- Tanaka A, Chiba K, Endoh T, Okuyama K, Kawahara A, Iida K, Tsukamoto N (2000) Low-noise readout circuit for uncooled infrared FPA. *Proc SPIE* 4130, Infrared Technol and Appl XXVI. <https://doi.org/10.1117/12.409858>

## Publisher's Note

Springer Nature remains neutral with regard to jurisdictional claims in published maps and institutional affiliations.